Automated extraction of phyllotactic traits from Arabidopsis thaliana

Timothée Wintz
wintz@csl.sony.fr
David Colliaux
colliaux@csl.sony.fr
Peter Hanappe
hanappe@csl.sony.fr

Sony CSL Paris
6, rue Amyot
75005 Paris

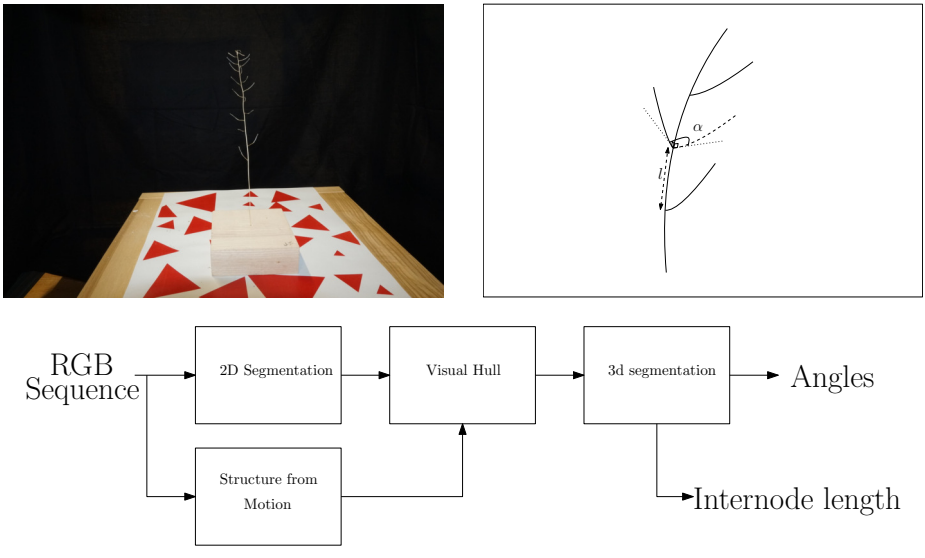

Figure 1: (Top left) Sample RGB image. (Top right) Measures of interest: angle between successive organs α; internode length l. (Bottom) Proposed processing pipeline.

1 Introduction

Large-scale phenotyping can help us understand biology but also to adapt cultures to a changing environment. Working on well understood model plants like arabidopsis can both provide useful data to the biologists and is an important stepping stone to the study of more complex models: in-field imaging of crops, imaging of plant populations...

Data collection and traits extractions are time-consuming process and a major bottleneck in plant phenotyping [13]. There is therefore a need of automated procedures to quickly

extract important parameters from live models. In this work, we propose a fully automated procedure to extract the structure of arabidopsis, including internode lengths and angles between successive organs.

In arabidopsis like in many other plants, the sequence of organs produce a Fibonacci spiral, each organ having an angle around the golden angle of 137.5° to the previous organ. Anomalies in these sequences are of particular interest to biologists, see for example [8].

The paper is structured as follows: section 2 reviews the related literature. Section 3 presents the general methodology and the hardware setup used in the experiments. Section 4 describes into details the different steps of the reconstruction procedure. Finally, section 5 validates the approach on both simulated and real world data.

2 Related works

As an answer to the need for computer vision in plant phenotyping, software have been made available for the analysis of 2d traits, like the open source Phenotiki [14] and PlantCV [6] including some machine learning aspects. It has also been pointed out in recent works that many of the current challenges are arising from 3d aspects of the morphology of plants [3].

There are already existing works on the 3d reconstruction of plants, including characterization of vegetation structure with a Kinect sensor [2] and phenotyping of sunflowers from 3D point clouds [7].

Arabidopsis is one of the most studied plants in biology, and has therefore been the subject to many works in computer vision for automatic phenotyping. These works include leaf surface reconstruction and growth monitoring [1, 9], branch angle estimation [4, 12].

To the authors' knowledge, no automated method for evaluation of the sequence of angles between successive organs has been presented yet. The originality of this work reside both in the fully automated aspect of the method, which require almost no specific tuning, and to the specific trait many biologists are interested in.

3 Acquisition method

3.1 General methodology

In this work, we present a method for the analysis of the phyllotaxis of arabidopsis from 2D images. More precisely, high resolution still RGB images of a single stem of Arabidopsis thaliana are taken along a circular trajectory around it. Visual markers are placed into the space to be enable the estimation of camera poses, and the background is black to allow for easy segmentation of the plant.

From this data, the goal is to segment organs from the stem, and to measure internode lengths and angles between successive organs. These angles are defined in the plane orthogonal to the stem (Fig. 1).

3.2 Hardware platform

For the experiments presented below, we use a home made solution as a 3D scanner. It consists in a X-Carve CNC Cartesian arm, combined with a pan-tilt gimbal with a camera mount. This setup therefore has five degrees of freedom. This gimbal can support different types of sensors. In this work, it consists in a Sony Alpha 5100 DSLR camera, remote

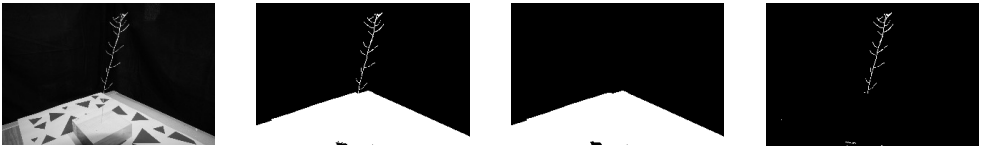

Figure 2: 2D Preprocessing steps. From left to right: original grayscale image, binary image, binary image on which the *open* filter has been applied, difference between the two previous images.

controlled with gphoto2. This allows for views from any point in space in a box containing the imaged plant. In addition to the additional degrees of freedom, another advantage of this platform compared to a rotating plate is the fact that the plant is not displaced. Therefore, there is less chance that the plant sways and it is easier to get a still plant in every frame.

4 Segmentation algorithm

In this section, we present the details of the reconstruction method from 2D images. The proposed pipeline is as follows (see figure 1): we first process the RGB images to obtain both a mask of the location of the plant and an estimation of the camera pose. Then from these, we compute the visual hull of the plant. This 3D volume is then processed further to estimate angles and internode lengths.

4.1 Pose estimation

The first step in our method consists in getting the camera poses from the pictures. To this end, we chose to use the result of a *Structure from motion (SfM)* algorithm, instead of a tedious calibration of our acquisition system. It is a well studied computer vision problem, for which many off-the-shelf commercial or open source solutions exist. For our experiments, we used the open source software *Colmap* [19, 20]. SfM rely on feature matching and do not work well in textureless pictures. Therefore, we used a sheet of paper with random patterns on the plane below the plant, as seen on figure 1.

From this SfM pipeline, we extract camera poses (camera extrinsics), the camera's fundamental matrix, and distortion coefficients which can be used to undistort images. From these parameters, any point in space can be projected onto all of the pictures.

4.2 2D Segmentation

To use the color image, the plant location must be identified and separated from the background in each frame. To this end, we apply a simple procedure to the input 2D images: first, we remove dark parts of the image by applying a threshold on pixel intensity. Second, we apply a morphology *open* filter to remove thin parts of the image, and then by applying the difference with the first binary image, we obtain the location of the branches. See figure 2 for an example of such a segmentation.

4.3 Visual Hull

The visual hull is a classical tool of 3D reconstruction from 2D images [10]. For a given set of 2D views of an object, its is defined as the set of all 3D points which projection in all views is inside the object. This volume contains all object points, and is in general a good approximation of the object shape if the number of views is sufficient. In the case of arabidopsis, which is a tree-like object, it is expected that the visual hull will be very close to the true shape of the object for a circular set of views around it.

To compute the visual hull, we use an approach similar to the one in [17]. This algorithm computes an octree in which each node is either labeled as *inside*, *outside*, or *inbetween* the visual hull. The nodes in the tree are split until either their size are smaller than the requested precision or the bounding region is either completely inside or outside the visual hull.

4.4 Skeletonization

In this subsection, we present a method to segment the plant, in the case of a single stem with thin organs along the stems. The first task is to separate the stem from the organs and to estimate the skeleton of the plant.

The visual hull octree can be converted in a 3D binary volume by splitting the cells to a fixed size, and subsequently filling the corresponding voxel positions. A skeleton is then computed using a thinning algorithm, which was introduced by [11]. An implementation from *scikit-learn* [16] was used to this end. This algorithm produces a thin set of voxels which approximate the medial axis of the visual hull. In the case of arabidopsis plants, this skeleton is a useful representation of the structure of the plant (Fig. 3).

From this thin structure, we build a graph which nodes are the positive voxels of our volume. Voxels are connected to all other voxels in a given radius, with edges oriented towards the top of the plant and weighted by distance. The constructed graph is therefore a directed acyclic graph, for which there exist efficient minimum spanning tree (MST) extraction algorithms, like Edmond's algorithm [5]. There may be artefacts in the reconstruction, thus there might be multiple weakly connected components. We select the largest one as the plant graph. We then compute the MST, and the stem is then segmented as the longest path in the graph. Then, the organs points are the weakly connected components of the MST in which we have removed the stem. We denote the set of points of the ith organ from the bottom of the plant by $\mathcal{F}_i$, for $1 \leq i \leq N_f$, where N_f is the number of organs.

4.5 Parameter estimation

We are interested in successive angles of the organs projected onto the plane orthogonal to the stem. Stretching the plants is a tedious work: to be able to use our method more effectively, it is important that the angle estimation also works if the stem is bent due to gravity. Therefore, we introduce the following method of angle estimation:

Let us assume that the stem points lie on a one-dimensional submanifold of $\mathbb{R}^3$, contained inside a euclidean plane $\mathcal{P}$. For any point p of the stem, let us denote the unit upwards tangent vector at p by t_p. Both $\mathcal{P}$ and t_p can be approximated using a principal component analysis (PCA). Let $\hat{\mathcal{P}}$ and $\hat{t}_p$ be such approximations of $\mathcal{P}$ and t_p respectively. Let us fix an arbitrary orientation for $\hat{\mathcal{P}}$.

We then define the following frame at p for any point p of the stem: let u_p be the orthogonal projection of $\hat{t}_p$ onto $\hat{\mathcal{P}}$. Let us complete (u_p) into a direct orthonormal basis (u_p, v_p) of

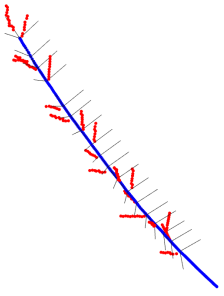

Figure 3: Segmented skeleton and projection planes. Stem points are in blue, organ points in red. Black lines represent basis vector on which organs are projected.

$\hat{\mathcal{P}}$. Finally, let us complete (u_p, v_p) into a direct orthonormal basis (u_p, v_p, w_p) of $\mathbb{R}^3$ (Fig. 3).

For $i \in \{1, \cdots, N_f\}$, let us define the following projection:

$$\begin{pmatrix} x \\ y \end{pmatrix} = \frac{1}{N_i} \sum_{j=1}^{N_i} \begin{pmatrix} v_p x_j - p \\ w_p y_j - q \end{pmatrix}, \tag{1}$$

where $\{(x_j, y_j), 1 \leq j \leq N_i\} = \mathcal{F}_i$ and (p,q) is the branching point between the organ $\mathcal{F}_i$ and the stem. We then define α_i, the angle for the ith organ, as the angle between $(1,0)$ and (x,y):

$$\alpha_i := \arctan2(y,x). \tag{2}$$

Internode length can simply be computed as the distance in the graph between successive branching nodes in the graph along the stem.

Other quantities such as organ length and angle between organ and stem can also be easily computed from the analysis, but are not included in the evaluation.

5 Results and evaluation

5.1 Simulated data

The algorithm was tested on a set of synthetic data generated using a simple model of arabidopsis main shoot and organs. The main shoot is modeled as a cylinder. A thin cylinder is used to model each peduncle and a slightly larger and longer cylinder is representing the organs attached to it. The organ and its peduncle are then attached along the main shoot. The parameters describing the model are:

- the length of the main shoot, peduncle and organ lengths and radii (L_s, L_p, L_f, R_s, R_p, R_f).
- the angle of organs relative to the main shoot (α_s).
- the internode I, that is the distance between two consecutive attachment points of the organs.

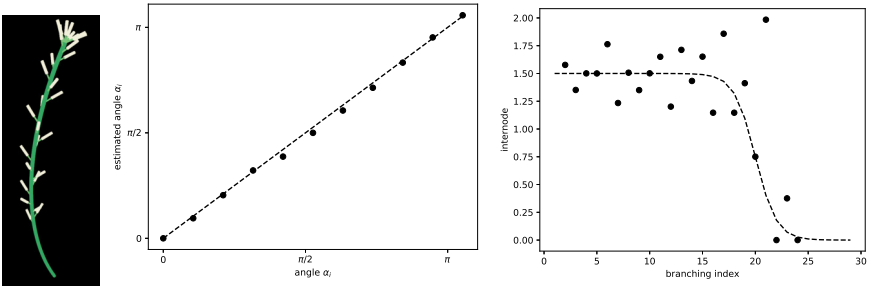

Figure 4: (Left) Rendered view of a model arabidopsis. (Center) Estimation of angle between 2 consecutive fruits α_i based on 100 views and voxel size of 2mm. (Right) Sequence of internodes as measured (dots) compared to the internodes imposed at generation (dashed line).

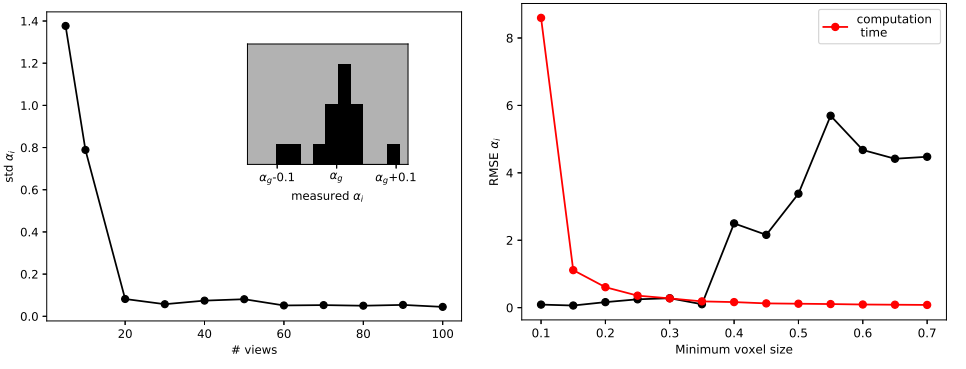

Figure 5: (Left) Standard deviation of the measured angles depending on the number of views considered to make the estimation. The insert shows a sample histogram when considering 100 views. (Right) RMSE of the estimated angles depending on the voxel size. We also report the computation time depending on the voxel size (arbitrary units) in red.

- the relative angle in the plane orthogonal to the main shoot between to consecutive organs (α_i)

Angles α_s and α_i are the same for all organs. The internode distance is modeled as a function of the distance of the attachment point from the main shoot terminal $I(z) = \frac{A}{1+e^{-a(z-b)}}$ in a similar fashion to what is reported about real plants in [15]. Views of the model were rendered along a circular trajectory around the plant using the Open3D [21] interface to OpenGL.

The angle estimation algorithm was evaluated on pairs of organs with various angles. A good accuracy of angle estimation and internode length can be achieved (Fig. 4).

The root mean square error (RMSE) of the measured angles are actually approximately constant if the number of views is more than a certain threshold (in our case, more than 20 views), and if the voxel size is greater than a certain size (in our case, around 0.35 (Fig 5). In real arabidopsis, variance around the golden angle is observed as around 20° [8] and

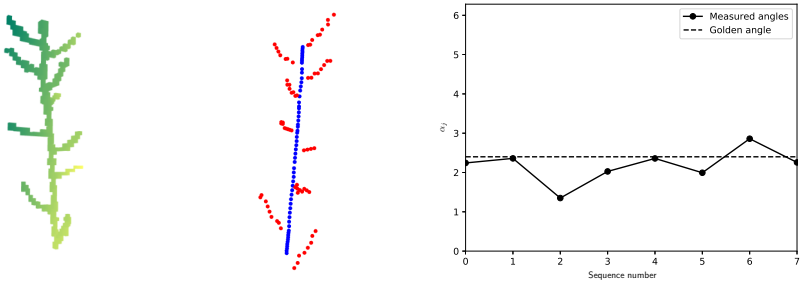

Figure 6: Reconstruction of a real arabidopsis. (Left) Visual hull with a voxel size of 2mm. (Center) Skeleton and segmented organs. (Right) Reconstructed angles.

the accuracy achieved by our method of less than 5° should therefore be more than precise enough to observe anomalies in angle sequences.

5.2 Real world example

To test our method on a real plant, we isolated a single stem of Arabidopsis thaliana and put it in a wooden stand (Fig. 1). From this plant, we took a series of 50 pictures around the plant using a Sony Alpha 5100 DSLR digital camera. The images were then downsampled from 6000x4000 resolution to 1500x1000 to reduce computation time.

Fig. 6 illustrates the result of the reconstruction from the RGB images presented in Fig. 1. The golden angle is plotted as a reference value: we can see that in this particular plant, the sequence presents no anomalies as all angles are close to the value of $\frac{2\pi}{\varphi^2} \simeq 2.40$ rad.

5.3 Computation time

Computations were done on a desktop computer with a single NVIDIA Titan X Pascal graphics card and a 3.20GHz Intel i5 CPU. In the real world example presented above, with image resolution of 1500x1000 and 50 images, *Colmap*'s structure from motion implementation takes a few seconds to complete, as well as 2D segmentation tasks. The most computationally expensive part of the algorithm is the computation of the visual hull, implemented in OpenCL, which takes 52 seconds for a voxel size of 1mm. This computing time could be further reduced, using more advanced space carving procedures, for example using integral images [18].

References

[1] Eren Erdal Aksoy, Alexey Abramov, Florentin Wörgötter, Hanno Scharr, Andreas Fischbach, and Babette Dellen. Modeling leaf growth of rosette plants using infrared stereo image sequences. *Computers and electronics in agriculture*, 110:78–90, 2015.

[2] George Azzari, Michael L Goulden, and Radu B Rusu. Rapid characterization of vegetation structure with a microsoft kinect sensor. *Sensors*, 13(2):2384–2398, 2013.

[3] Alexander Bucksch, Acheampong Atta-Boateng, Akomian F Azihou, Dorjsuren Battogtokh, Aly Baumgartner, Brad M Binder, Siobhan A Braybrook, Cynthia Chang, Viktoirya Coneva, Thomas J DeWitt, et al. Morphological plant modeling: unleashing geometric and topological potential within the plant sciences. *Frontiers in plant science*, 8:900, 2017.

[4] Sruti Das Choudhury, Saptarsi Goswami, Srinidhi Bashyam, Ashok Samal, and Tala Awada. Automated stem angle determination for temporal plant phenotyping analysis. In *Computer Vision Workshop (ICCVW), 2017 IEEE International Conference on*, pages 2022–2029. IEEE, 2017.

[5] Yoeng-Jin Chu. On the shortest arborescence of a directed graph. *Science Sinica*, 14: 1396–1400, 1965.

[6] Noah Fahlgren, Maximilian Feldman, Malia A Gehan, Melinda S Wilson, Christine Shyu, Douglas W Bryant, Steven T Hill, Colton J McEntee, Sankalpi N Warnasooriya, Indrajit Kumar, et al. A versatile phenotyping system and analytics platform reveals diverse temporal responses to water availability in setaria. *Molecular plant*, 8(10): 1520–1535, 2015.

[7] William Gélard, Michel Devy, Ariane Herbulot, and Philippe Burger. Model-based segmentation of 3d point clouds for phenotyping sunflower plants. In *12th International Joint Conference on Computer Vision, Imaging and Computer Graphics Theory and Applications (VISAPP 2017)*, volume 4, pages 459–467, 2017.

[8] Yann Guédon, Yassin Refahi, Fabrice Besnard, Etienne Farcot, Christophe Godin, and Teva Vernoux. Pattern identification and characterization reveal permutations of organs as a key genetically controlled property of post-meristematic phyllotaxis. *Journal of theoretical biology*, 338:94–110, 2013.

[9] Eli Kaminuma, Naohiko Heida, Yuko Tsumoto, Naoki Yamamoto, Nobuharu Goto, Naoki Okamoto, Akihiko Konagaya, Minami Matsui, and Tetsuro Toyoda. Automatic quantification of morphological traits via three-dimensional measurement of arabidopsis. *The Plant Journal*, 38(2):358–365, 2004.

[10] Aldo Laurentini. The visual hull concept for silhouette-based image understanding. *IEEE Transactions on pattern analysis and machine intelligence*, 16(2):150–162, 1994.

[11] Ta-Chih Lee, Rangasami L Kashyap, and Chong-Nam Chu. Building skeleton models via 3-d medial surface axis thinning algorithms. *CVGIP: Graphical Models and Image Processing*, 56(6):462–478, 1994.

[12] Lu Lou, Yonghuai Liu, Minglan Shen, Jiwan Han, Fiona Corke, and John H Doonan. Estimation of branch angle from 3d point cloud of plants. In *3D Vision (3DV), 2015 International Conference on*, pages 554–561. IEEE, 2015.

[13] Massimo Minervini, Hanno Scharr, and Sotirios A Tsaftaris. Image analysis: the new bottleneck in plant phenotyping [applications corner]. *IEEE signal processing magazine*, 32(4):126–131, 2015.

[14] Massimo Minervini, Mario V Giuffrida, Pierdomenico Perata, and Sotirios A Tsaftaris. Phenotiki: an open software and hardware platform for affordable and easy image-based phenotyping of rosette-shaped plants. *The Plant Journal*, 90(1):204–216, 2017.

[15] Lars Mündermann, Yvette Erasmus, Brendan Lane, Enrico Coen, and Przemyslaw Prusinkiewicz. Quantitative modeling of arabidopsis development. *Plant Physiology*, 139(2):960–968, 2005. ISSN 0032-0889. doi: 10.1104/pp.105.060483. URL http://www.plantphysiol.org/content/139/2/960.

[16] F. Pedregosa, G. Varoquaux, A. Gramfort, V. Michel, B. Thirion, O. Grisel, M. Blondel, P. Prettenhofer, R. Weiss, V. Dubourg, J. Vanderplas, A. Passos, D. Cournapeau, M. Brucher, M. Perrot, and E. Duchesnay. Scikit-learn: Machine learning in Python. *Journal of Machine Learning Research*, 12:2825–2830, 2011.

[17] Michael Potmesil. Generating octree models of 3d objects from their silhouettes in a sequence of images. *Computer Vision, Graphics, and Image Processing*, 40(1):1–29, 1987.

[18] Hanno Scharr, Christoph Briese, Patrick Embgenbroich, Andreas Fischbach, Fabio Fiorani, and Mark Müller-Linow. Fast high resolution volume carving for 3d plant shoot reconstruction. *Frontiers in plant science*, 8:1680, 2017.

[19] Johannes Lutz Schönberger and Jan-Michael Frahm. Structure-from-motion revisited. In *Conference on Computer Vision and Pattern Recognition (CVPR)*, 2016.

[20] Johannes Lutz Schönberger, Enliang Zheng, Marc Pollefeys, and Jan-Michael Frahm. Pixelwise view selection for unstructured multi-view stereo. In *European Conference on Computer Vision (ECCV)*, 2016.

[21] Qian-Yi Zhou, Jaesik Park, and Vladlen Koltun. Open3D: A modern library for 3D data processing. *arXiv:1801.09847*, 2018.